RSC Advances

ROYAL SOCIETY OF CHEMISTRY

www.rsc.org/advances

Cite this: DOI: 10.1039/c0xx00000x

www.rsc.org/xxxxxx

ARTICLE TYPE

Freestanding 3D Graphene/Cobalt Sulfide Composites for Supercapacitors and Hydrogen Evolution Reaction

Yang Wang, Jing Tang, Biao Kong, Dingsi Jia, Yuhang Wang, Tiance An, Lijuan Zhang,* and Gengfeng Zheng*

Received (in XXX, XXX) Xth XXXXXXXXX 20XX, Accepted Xth XXXXXXXXX 20XX
DOI: 10.1039/b000000x

The development of lightweight, flexible, electrochemically active materials with high efficiency is important for energy storage and conversion. In this study, we report the fabrication of a freestanding, 3-dimensional graphene/cobalt sulfide nanoflake (3DG/CoS_x) composite for supercapacitors and hydrogen evolution catalysts. The graphene framework formed by chemical vapour deposition provides superlight, highly conductive electron transport pathways, as well as abundant pores for electrolyte penetration. The densely patterned cobalt sulfide nanoflake arrays grown by electrodeposition offer large surface area for electrochemical reactions, high theoretical capacitance and efficient hydrogen evolution catalytic activity. As proofs-of-concept, supercapacitors made of the 3DG/CoS_x composites deliver a high specific capacitance of 443 F/g at 1 A/g, with excellent capacity retention of 86% after 5000 cycles and mechanical flexibility. In addition, the 3DS/CoS_x composites show attractive features as hydrogen evolution catalysts, with a low overpotential of 0.11 V and a Tafel slope of 93 mV/dec.

Introduction

The fast increase in the global energy demand has been driving the research exploration of new materials and technologies that enable robust and simple design, high efficiency, and low cost.[1-8] Cobalt sulfides (CoS_x), due to their high potentials in electrochemical supercapacitors,[9] Li-ion rechargeable batteries,[10,11] and heterogeneous electrocatalysis such as hydrogen evolution reaction (HER),[12] have been recently attracting substantial interest. The synthesis of a variety of CoS_x nanostructures, including nanowire,[13] nanotubes,[14] nanosheets,[15] flowers,[9, 16] hollow spheres [17, 18] and ellipsoids [19] have been demonstrated. In addition, conducting materials are often incorporated to enhance the intrinsically poor electrical conductivity of CoS_x.[17] For instance, the composites of hydrothermally synthesized CoS_x nanoparticles and graphene thin films on Ni films have been demonstrated with excellent supercapacitor performance of 1535 F/g at 2 A/g.[20] The electrodeposition of CoS_x nanosheets on Ni foams has also been reported with a high specific capacitance of 1471 F/g at 4 A/g.[15] Nonetheless, the low percentage of the electrochemically active materials compared to the electrode substrate (e.g. CoS_x vs. Ni film) has limited the potential applications of these materials in super-light, flexible electrodes with excellent energy performances.

In contrast to conventional electrodes, the freestanding, 3-dimensional graphene (3DG) frameworks, produced by chemical vapour deposition (CVD),[21] enable several attractive features of low density (57 mg/cm^3, compared to 347 mg/cm^3 for commercial carbon cloth),[22] superior electrical conductivity (~1.3 × 10^5 S/m at 300 K),[23] high mechanical flexibility and chemical stability,[24] which may allow for more attractive performances as a kind of superlight electrode materials than carbon fibers,[22] porous carbon thin films,[25] reduced graphene oxide[26] and graphene-conducting polymer composites.[27] A variety of materials, including Co_3O_4 nanowires,[28] MnO_2 nanoparticles,[29] and MoS_2[30] have been investigated for the direct growth or loading on these 3DG frameworks for energy storage applications. On the other hand, in spite of their high potentials in energy storage and conversion, the direct growth of CoS_x nanostructures on freestanding 3DG frameworks, preferably with large surface area and high electrocatalytic activity, has not been achieved yet.

Herein, we demonstrate the fabrication of a freestanding 3DG/CoS_x nanosheet composite, with excellent supercapacitor performance and HER catalytic activity. CoS_x nanosheets are first electrodeposited onto the CVD-grown, Ni-catalyzed 3DG frameworks, followed by etching of the supporting Ni foam to obtain the freestanding composites. The electrodeposition is facile and well-controlled, and allows for strong attachment of CoS_x onto the CVD-grown graphene without additional hydrophilic surface pre-treatment. The loading mass ratio of CoS_x is ~24%, significantly higher than that of CoS electrodeposited on Ni foams (ca. < 1%).[15] In addition, the 2-dimensional (2D) CoS_x nanosheet arrays provide a high surface area for electrochemical

reactions, and space for efficient electrolyte diffusion. Meanwhile, the supporting 3DG framework offer fast charge transport pathways, structural flexibility for mechanical stress, and light weight. As proofs-of-concept, supercapacitors made of these freestanding 3DG/CoS_x composites have shown a high reversible specific capacitance of 443 F/g at a current density of 1 A/g, (or 106 F/g with respect to the entire electrode mass), which is maintained with excellent cycling stability (~ 86%) after 5000 cycles. Moreover, these freestanding 3DG/CoS_x composites have also exhibited attractive potential as HER catalysts, with a low onset potential of –110 mV vs. RHE that is comparable to Pt, and a high on-current density of 82.24 A/g (or 36.65 A/g with respect to the entire electrode mass) at –0.39 V vs. RHE.

Experimental

Synthetic procedures

All chemicals used in this work were analytical, commercial available and without further purification. The 3DG thin films were synthesized by chemical vapour deposition using Ni foams as growth substrate and catalysts according to the literature.[21] Briefly, Ni foams (~ 0.5 mm thick) were firstly folded into 2 layer (200 mm×104 mm) and then pressed into a thin sheet~0.3 mm thick.[29] After pre-treatments, the pressed nickel foams were prepared to grow graphene at 1000 °C in a horizontal tube furnace under Ar (500 s.c.c.m.), H_2 (200 s.c.c.m.) and CH_4 (10 s.c.c.m) for 5 min. After growth, the graphene/Ni foams were cut into 20 mm×40 mm small pieces which were further coated with PMMA before etched by HCl. Next, PMMA was removed after the Ni foams were etched completely and finally, the freestanding 3DG was obtained.

In order to avoid damaging the structure of 3D graphene networks, a copper wire was connected to 3D graphene networks with silver paste protected by covering epoxide-resin glue. The electrodeposition of CoS_x was modified according to the literature. [15] In brief, a piece of 3D graphene network was immersed into the aqueous solution containing 5 mM $CoCl_2.6H_2O$ and 0.75 M thiourea. The electrochemical deposition was performed with a three-electrode setup, where the conductive 3D graphene network was employed as the working electrode, a platinum electrode and an Ag/AgCl electrode as the counter electrode and the reference electrode, respectively. The sweep potential interval for potentiodynamic deposition was performed using a CHI660 electrochemical workstation (CH Instruments, USA). After electrodeposition, the composite was taken out and rinsed with deionized water to remove excess electrolyte, and then dried in a vacuum oven at 80 °C overnight.

The two synthesis procedures above-mentioned show in the schematic illustration (**Fig. 1**).

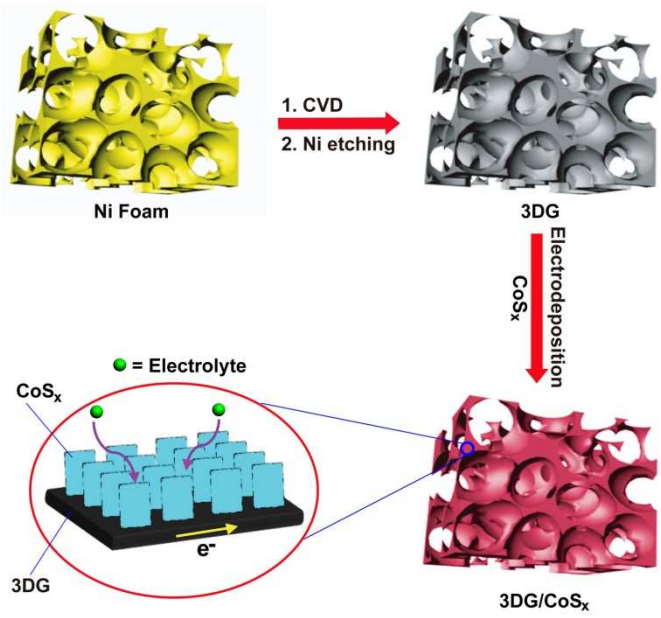

Fig. 1 Schematic illustration of synthesis process of the freestanding 3DG/CoS_x nanoflake composite electrode.

Electrochemistry characterization

The electrochemical performance measurements were conducted on a CHI660D electrochemical workstation, with a three-electrode configuration at room temperature using 1.0 M KOH as the electrolyte. The 3DG/CoS_x composite in contact with a Cu wire by silver paint and epoxy resin was directly used as a working electrode. A platinum wire and an Ag/AgCl electrode were used as the counter and the reference electrodes, respectively.

Results and Discussion

Morphology and structural characterization

The fabrication of freestanding 3DG/CoS_x composites is schematically shown in **Fig. 1**. A Ni foam with 3D architecture and macropores is first used as both the substrate and catalyst for the CVD deposition of graphene, followed by the Ni etched to obtain the freestanding 3DG framework. It can be clearly seen that the film is changed from the original shinning bright colour to dark gray after the 3DG deposition, while the size and morphology of the whole film remain almost unaltered (**Fig. S1**). The size of the obtained 3DG film can reach hundreds of square centimetres, and is readily scaled up with larger CVD quartz tube sizes. The mass loading of 3DG deposited on Ni foam is nearly linear with the reaction time from 2 to 20 min with a growth rate ~0.047 mg/(cm^2·min) (**Fig. S2a**). After acid treatment, the lightweight, dark gray, freestanding 3DG thin film is obtained, which is then directly used as the electrode and substrate for the electrodeposition of CoS_x. After the electrodeposition, the 3DG surface is uniformly covered with a black thin layer (**Fig. 2a**).

The mass loading of CoS_x is almost linearly dependent on the electrodeposition cycle numbers at a deposition rate of 0.021 mg/cm^2 per cycle (**Fig. S2b**).

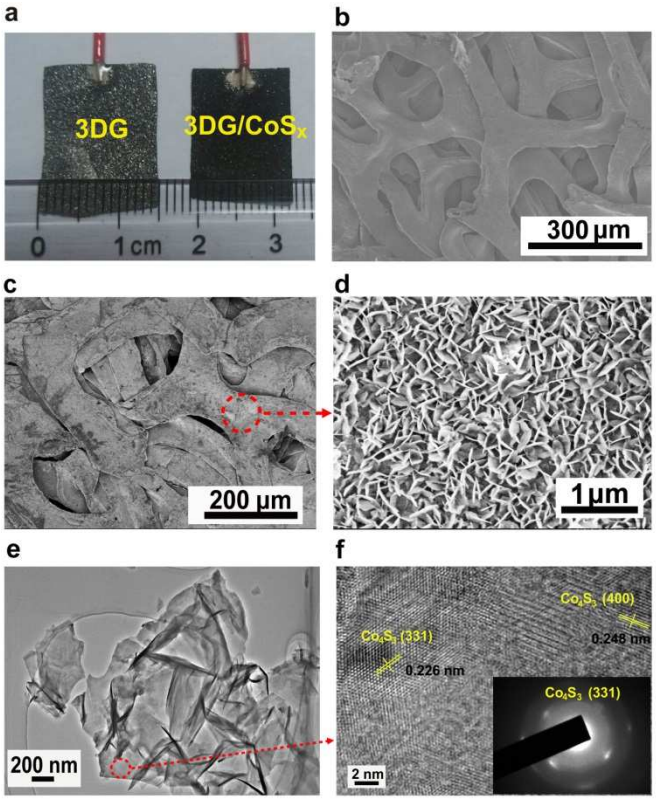

Fig. 2. (a) Digital photograph of bare 3DG and 3DG/CoS_x electrodes (Left: Bare 3DG; Right: 3DG/CoS_x). **(b)** SEM images of bare 3DG skeleton and **(c)** 3DG/CoS_x skeleton. **(d)** SEM image of the as-synthesized nanoflake-like CoS_x. **(e)** TEM image and **(f)** HRTEM image of CoS_x nanoflakes. (Inset: SAED pattern of CoS_x nanoflake).

Scanning electron microscopy (SEM) images show that the 3DG frameworks completely replicate the Ni foam skeleton, with an average mesh size is about 200 μm (**Fig. 2b**). The surface of the 3DG frameworks is covered with a dense layer of CoS_x 2D nanoflakes, with orientation nearly perpendicular to the underlying graphene substrate (**Fig. 2c, d**). Transmission electron microscopy (TEM) images show that these nanoflakes have an ultralow thickness, with an average edge length of ~500 nm. High-resolution TEM (HRTEM) images clearly exhibit several lattice spacings of 0.226 and 0.248 nm, which correspond to the interspacings of the (331) and (400) planes of Co_4S_3, respectively (PDF#02-1338) (**Fig. 2f**). The selected area electron diffraction (SAED) pattern demonstrates that the obtained CoS_x nanoflakes are crystalline and the inner ring is in line with the (331) plane of Co_4S_3 (**Fig. 2f**, inset).

Raman spectroscopy characterization show that the freestanding 3DG thin films have two sharp peaks at ~ 1581 and 2687 cm^{-1} (**Fig. 3a**), corresponding to the G and 2D peaks of graphene, respectively.[28] There is no obvious graphene D band at ~1350 cm^{-1}, suggesting the high quality of the as-prepared 3DG thin films.[28] X-ray diffraction (XRD) pattern of the 3DG thin film reveals two significant peaks at 2θ = 26.5° and 54.6° (**Fig. 3b**), attributed to the (002) and (004) reflections of graphic carbon, respectively (JCPDS 75-1621). No XRD peaks are attributed to CoS_x, which can be ascribed to the low crystallinity of the as-made CoS_x nanoflakes. X-ray photoelectron spectroscopy (XPS) measurements are carried out to confirm the chemical composition of CoS_x. The two main peaks, located at 780.8 and 796.7 eV, and a shake-up feature at higher binding energies are attributed to Co^{2+} in CoS_x (**Fig. 3c**).[9,31]The binding energy value of the main peak of S2p is ~ 162.9 eV (**Fig. 3d**), consistent with that of CoS reported previously,[13] indicating that most of the S species exist as S^{2-}. The peak at 168 eV is attributed to sulfur oxides generated in the electrodeposition process.[15]

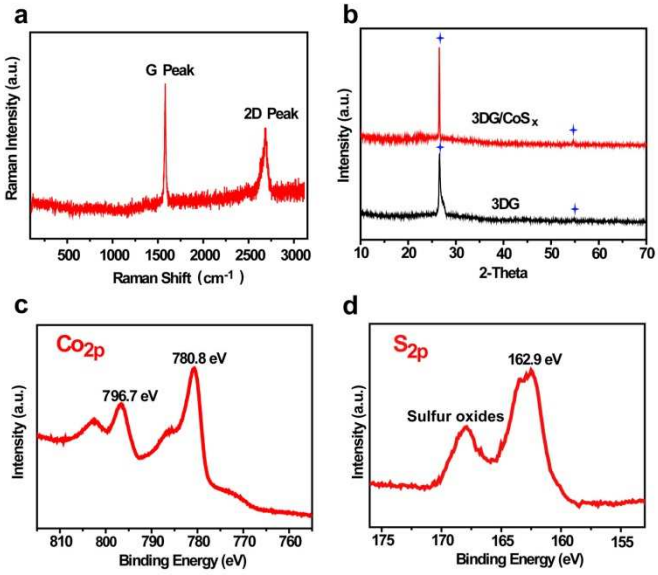

Fig. 3. Raman spectra **(a)** and XRD pattern **(b)** of 3DG. XPS spectra of **(c)** Co_{2p} and **(d)** S_{2p} of the nanoflake-like CoS_x electrode.

Electrochemical properties and HER catalytic activity of 3DG/CoS_x

The electrochemical performances of the freestanding 3DG/CoS_x composites are studied in 1 M KOH aqueous electrolyte. The cyclic voltammetry (CV) curves are measured over a voltage range from −0.2 to 0.6 V for the 3DG/CoS_x composites at a scan rate of 20 mV/s (**Fig. 4a**). Compared to the freestanding 3DG sample, the CV curve of the 3DG/CoS_x composites is substantially increased, suggesting that a large specific capacitance is attributed to the growth of the electroactive CoS_x nanoflakes, instead of the double-layer capacitance of the original 3DG. Two peaks of redox pairs are observed: O_1 vs. R_1, and O_2 vs. R_2, which are attributed to the conversion between Co (II) and Co (III), and Co (III) to Co (IV), respectively.[32] The electrochemical process of the 3DG/CoS_x composites is then investigated by CV tests between −0.2 to 0.6 V at different scan rates from 10 to 100 mV/s (**Fig. 4b**). Both the CV curves' area and the redox peaks' height are increased with the scan rate, indicating the fast redox reaction rates of the 3DG/CoS_x composites. While inferior performances are shown

when 3DG is removed (**Figure S3**), with smaller CV curves' area and lower specific capacitance about 77 F/g at 1 A/g. A good linear relationship between the peak current densities and the square root of scan rate further demonstrates a good rate capability of the 3DG/CoS_x electrode (**Fig. 4c**).

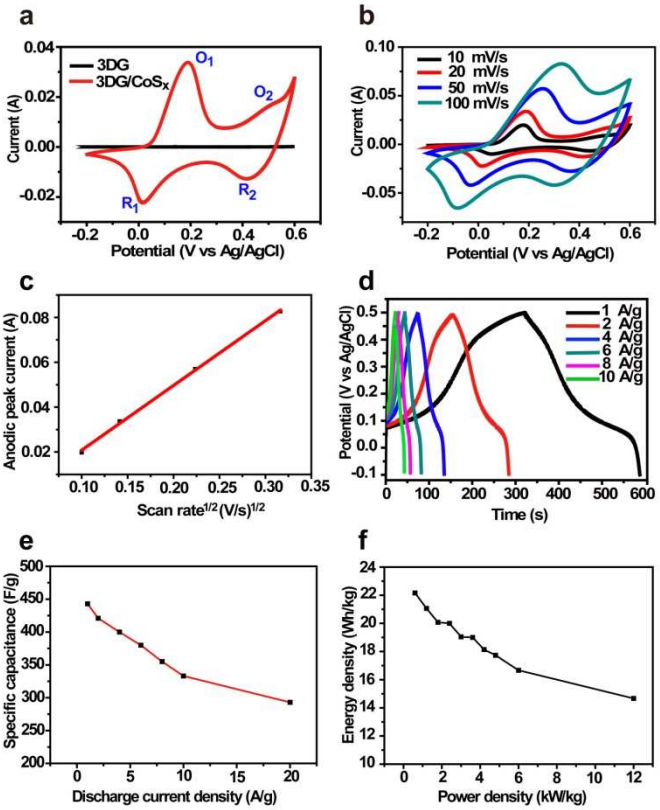

Fig. 4. Electrochemical performance of the 3D graphene electrodes measured in 1.0 M KOH aqueous electrolyte. **(a)** CV curves of bare 3DG (the black line) and 3DG/CoS_x composite electrode (the red line) measured at a scan rate of 20 mV/s. **(b)** CV curves of 3DG/CoS_x composite electrode at different potential scan rates. **(c)** The resultant anodic current peak current density dependence of the scan rate calculated from **Fig. 2b**. **(d)** Galvanostatic charge-discharge curves of 3DG/CoS_x composite electrode at various current densities. **(e)** Specific capacitance of 3DG/CoS_x composite electrode at different charge-discharge rates. **(f)** Ragone plot of the estimated energy density and power density of 3DG/CoS_x composite electrode.

The charge-discharge behaviors of the 3DG/CoS_x composites are further investigated under a chronopotentiometry mode, which shows typical triangular shapes (**Fig. 4d**). When only the mass of CoS_x is used for calculation, the specific capacitance of the 3DG/CoS_x composites is measured as 443, 400, 380, 355, 333, and 293 F/g, at the current densities of 1, 4, 6, 8,10 and 20 A/g, respectively (**Fig. 4e**). Although these capacitances are lower than that of CoS_x grown on Ni foams reported previously (1471 F/g at 4 A/g),[15] due to the relatively lower conductivity of 3DG than Ni foams, the ultralight weight of the freestanding 3DG provides an attractive feature for the specific capacitance of the whole electrode (including both CoS_x and the supporting 3DG). For instance, taking account into the 25% weight percentage of CoS_x of the total 3DG/CoS_x composite, the specific capacitances are 106 and 70 F/g at 0.24 and 5 A/g, respectively, better than or comparable to the best specific capacitance reported previously for the whole electrode (e.g. 130 F/g for freestanding 3DG/MnO_2).[29] Moreover, the Ragone plot of the freestanding 3DG/CoS_x composites shows that with the increase of power density from 0.6 to 12 kW/kg, the energy density change from 22 to 15 Wh/kg (**Fig. 4f**). A high power density of 12 kW/kg and a high energy density of 22 Wh/kg are obtained at fast and slow charge/discharge rates, respectively.

The cycling stability of the freestanding 3DG/CoS_x composites is further examined at a current density of 2 A/g. The charge/discharge curves of the composites are maintained with a symmetric shape over a long period (>10^6 s) of charge-discharge time (**Fig. 5a**). The specific capacitance is retained at ~ 90% after 5000 charge/discharge cycles (**Fig. 5b**, red curve), substantially higher than previous report of the CoS nanocages (70.3% after 3000 cycles).[33] The Coulombic efficiency is increased from the initial 89% to 98% at ~ the 1000th cycle, and is well maintained afterwards with slight change of CoS_x nano-flake morphology after 5000 cycles (**Figure S4a**). In addition, the CV curves of the freestanding 3DG/CoS_x composites are almost overlapped with each other after repeated folding and extending for tens of times (**Fig. 5c**), suggesting the good mechanical stability and flexibility of the composites. Moreover, Nyquist plots obtained from the electrochemical impedance spectroscopy (EIS) show that the 3DG/CoS_x composites have a smaller equivalent series resistance (1.2 Ω) than that of the CoS_x powder (10.6 Ω) (**Fig. 5d**), indicating that 3DG is highly conductive and serve as the main charge transport pathways.

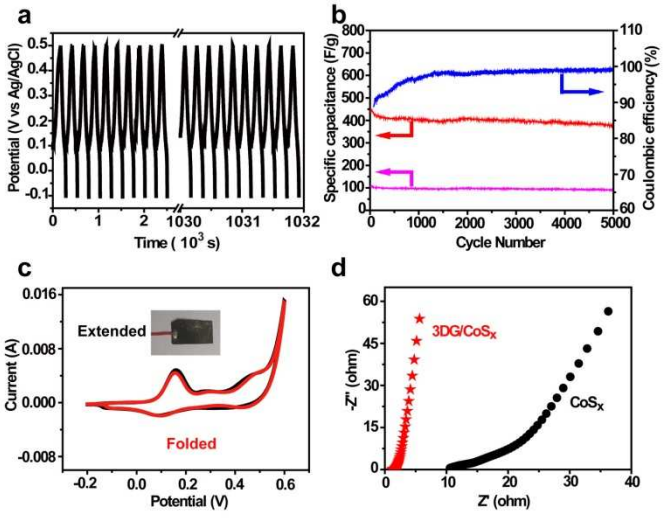

Fig. 5 (a) Charge/discharge profile of the composite electrode at a current density of 2.0 A/g. **(b)** Cycling performance of 3DG/CoS_x composite electrode at a current density of 2.0 A/g (the blue curve: coulombic efficiency of 3DG/CoS_x; the red curve: specific capacitance calculated from CoS_x only; the pink curve: specific capacitance calculated from the 3DG/CoS_x entire electrode). **(c)** CV curves of 3DG/CoS_x before and after repeated folding with an angle of almost 180°C at a scan rate of 5 mV/s

(d) Nyquist plots of CoS_x and the 3DG/CoS_x composite electrode .

Finally, the potential of using the freestanding 3DG/CoS_x composites as HER catalysts is investigated in a PBS (Phosphate Buffered Saline) electrolyte solution. Compared to the 3DG substrate with almost no HER activity, the 3DG/CoS_x composites exhibit a low onset potential of -0.11V, and a high current density of 13.34 mA/cm^2 at -0.4 V vs. RHE (**Fig. 6a**). This low onset potential is almost the same as the best reported HER activity for CoS_x structures under similar conditions,[12] and close to that of Pt.[34] A Tafel slope of 93 mV/dec is obtained, also comparable to the best reported results [12] (**Fig. 6a**, inset). Repeated scans of the freestanding 3DG/CoS_x composites show that the current density drops ~ 30% from the 1st to the 1000th scan cycles, suggesting a good electrochemical stability of the composite (**Fig. 6b**). The durability of the 3DG/CoS_x in neutral pH water is further measured in a longer-duration controlled potential electrolysis test (**Fig. S5**). The 3DG/CoS_x provides a good HER activity, with ~ 25% loss in activity over 24 h. In contrast, when a blank 3DG is employed as the working electrode under the same conditions, the current density is negligible but not zero, which may be due to the residues of Ni particles in 3DG skeleton.[35] A clear change of the CoS_x morphology is observed after 24 h of controlled potential electrolysis test (**Fig. S4b**).

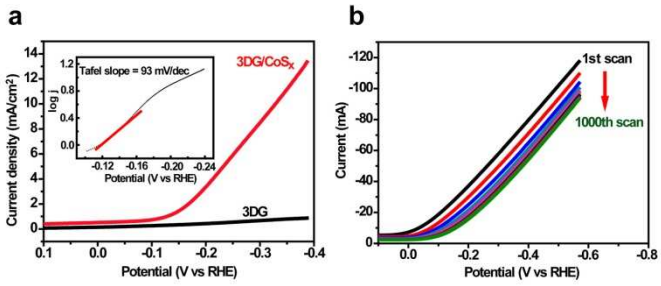

Fig. 6 (a) Polarization curves of 3DG(black line) and 3DG/CoS_x (red line) in 1MPBS at scan rate: 5 mV/s (inset: Tafel plot derivatized from the polarization curve of 3DG/CoS_x. **(b)** Polarization curves of 3DG/CoS_x from 1st to 1000th scan.

Our 3DG/CoS_x has shown its potential of serving as an good candidate for supercapacitors. As mentioned above, the 3DG/CoS_x achieves a high specific capacitance of 443 F/g and specific capacitance retention of 86%, which are comparable or better than most of the previous reports (Table S1). In addition, its flexible and lightweight features can allow for new opportunities for the future development of energy storage devices. Furthermore, the 3DG/CoS_x can also serve as an excellent HER catalyst with a Tafel slope of 93 mV/dec, demonstrating its potential of combing energy storage and conversion for next-generation multifunctional energy devices.

Conclusions

In summary, we have successfully prepared a freestanding, lightweight and flexible 3DG/CoS_x composites for energy storage and conversion. The lightweight 3D graphene network are thermally grown from Ni foams, followed by etching of Ni foam and subsequent electrodeposition of CoS_x nanoflakes to obtain the freestanding 3DG/CoS_x composites. The densely packed CoS_x nanoflakes provide high surface area and electrochemically reactive surface, and the freestanding 3DG framework allows for efficient charge transport pathways. As a proof-of-concept, the electrode made of the 3DG/CoS_x composites possess remarkable electrochemical performances, with a high specific capacitance, excellent cycling stability and mechanical stability. Due to its light weight, the total electrode (including the 3DG substrate) even delivers a high specific capacitance of 106 F/g, which is more than those using metal substrates as current collectors. Moreover, the freestanding 3DG/CoS_x composites also exhibit a low onset potential and high current density for HER activity. Taking together, the freestanding 3DG/CoS_x composites show substantial potential for next-generation light-weight, high-performance energy storage and conversion.

Acknowledgements

We thank the following funding agencies for supporting this work: the National Key Basic Research Program of China (2013CB934104), the Natural Science Foundation of China (21322311, 21473038, 21071033, 21471034), the Science and Technology Commission of Shanghai Municipality (14JC1490500), the Doctoral Fund of Ministry of Education of China (20130071110031), the Program for Professor of Special Appointment (Eastern Scholar) at Shanghai Institutions of Higher Learning, and the Deanship of Scientific Research of King Saud University (IHCRG#14-102).

Notes and references

[a] Laboratory of Advanced Materials, Department of Chemistry, Fudan University, Shanghai 200433, People's Republic of China; E-mail: gfzheng@fudan.edu.cn.

† Electronic Supplementary Information (ESI) available: [Electrode preparation, digital photos, and plots]. See DOI: 10.1039/b000000x/

1. M. Beidaghi and Y. Gogotsi, *Energy Environ. Sci.*, 2014, **7**, 867-884.
2. X. Wang, X. Lu, B. Liu, D. Chen, Y. Tong and G. Shen, *Adv. Mater.*, 2014, **26**, 4763-4782.
3. M.-R. Gao, Y.-F. Xu, J. Jiang and S.-H. Yu, *Chem. Soc. Rev.*, 2013, **42**, 2986-3017.
4. L. Liu, Z. Niu, L. Zhang, W. Zhou, X. Chen and S. Xie, *Adv. Mater.*, 2014, **26**, 4855-4862.
5. G. Q. Zhang, H. B. Wu, H. E. Hoster and X. W. Lou, *Energy Environ.Sci.*, 2014, **7**, 302-305.
6. Y. Tang, Y. Zhang, J. Deng, D. Qi, W. R. Leow, J. Wei, S. Yin, Z. Dong, R. Yazami, Z. Chen and X. Chen, *Angew. Chem. Int. Ed.*, 2014.
7. L. Mai, X. Tian, X. Xu, L. Chang and L. Xu, *Chem. Rev.*, 2014.
8. Y. Cheng, H. Zhang, C. V. Varanasi and J. Liu, *Energy Environ. Sci.*, 2013, **6**, 3314-3321.

9. F. Luo, J. Li, H. Yuan and D. Xiao, *Electrochim. Acta*, 2014, **123**, 183-189.
10. W. Shi, J. Zhu, X. Rui, X. Cao, C. Chen, H. Zhang, H. H. Hng and Q. Yan, *ACS Appl. Mater. Interfaces*, 2012, **4**, 2999-3006.
11. S. Liu, J. Wang, J. Wang, F. Zhang, F. Liang and L. Wang, *CrystEngComm*, 2014, **16**, 814-819.
12. Y. Sun, C. Liu, D. C. Grauer, J. Yano, J. R. Long, P. Yang and C. J. Chang, *J. Am. Chem. Soc.*, 2013, **135**, 17699-17702.
13. X. Xia, C. Zhu, J. Luo, Z. Zeng, C. Guan, C. F. Ng, H. Zhang and H. J. Fan, *Small*, 2014, **10**, 766-773.
14. J. Pu, Z. Wang, K. Wu, N. Yu and E. Sheng, *Phys. Chem. Chem. Phys.*, 2014, **16**, 785-791.
15. J.-Y. Lin and S.-W. Chou, *RSC Adv.*, 2013, **3**, 2043-2048.
16. Q. Wang, L. Jiao, H. Du, W. Peng, Y. Han, D. Song, Y. Si, Y. Wang and H. Yuan, *J. Mater. Chem.*, 2011, **21**, 327-329.
17. Q. Wang, L. Jiao, H. Du, Y. Si, Y. Wang and H. Yuan, *J. Mater. Chem.*, 2012, **22**, 21387-21391.
18. Q. Wang, L. Jiao, Y. Han, H. Du, W. Peng, Q. Huan, D. Song, Y. Si, Y. Wang and H. Yuan, *J. Phys. Chem. C*, 2011, **115**, 8300-8304.
19. L. Zhang, H. B. Wu and X. W. Lou, *Chem. Commun.*, 2012, **48**, 6912-6914.
20. B. H. Qu, Y. J. Chen, M. Zhang, L. L. Hu, D. N. Lei, B. A. Lu, Q. H. Li, Y. G. Wang, L. B. Chen and T. H. Wang, *Nanoscale*, 2012, **4**, 7810-7816.
21. Z. Chen, W. Ren, L. Gao, B. Liu, S. Pei and H.-M. Cheng, *Nat. Mater.*, 2011, **10**, 424-428.
22. L. Yuan, X.-H. Lu, X. Xiao, T. Zhai, J. Dai, F. Zhang, B. Hu, X. Wang, L. Gong, J. Chen, C. Hu, Y. Tong, J. Zhou and Z. L. Wang, *ACS Nano*, 2011, **6**, 656-661.
23. J. Ji, L. L. Zhang, H. Ji, Y. Li, X. Zhao, X. Bai, X. Fan, F. Zhang and R. S. Ruoff, *ACS Nano*, 2013, **7**, 6237-6243.
24. B. G. Choi, S. J. Chang, H. W. Kang, C. P. Park, H. J. Kim, W. H. Hong, S. Lee and Y. S. Huh, *Nanoscale*, 2012, **4**, 4983-4988.
25. Y. Li, J. Chen, L. Huang, C. Li, J.-D. Hong and G. Shi, *Adv. Mater.*, 2014, **26**, 4789-4793.
26. C.-B. Ma, X. Qi, B. Chen, S. Bao, Z. Yin, X.-J. Wu, Z. Luo, J. Wei, H.-L. Zhang and H. Zhang, *Nanoscale*, 2014, **6**, 5624-5629.
27. Q. Wu, Y. Xu, Z. Yao, A. Liu and G. Shi, *ACS Nano*, 2010, **4**, 1963-1970.
28. X.-C. Dong, H. Xu, X.-W. Wang, Y.-X. Huang, M. B. Chan-Park, H. Zhang, L.-H. Wang, W. Huang and P. Chen, *ACS Nano*, 2012, **6**, 3206-3213.
29. Y. He, W. Chen, X. Li, Z. Zhang, J. Fu, C. Zhao and E. Xie, *ACS Nano*, 2012, **7**, 174-182.
30. X. Cao, Y. Shi, W. Shi, X. Rui, Q. Yan, J. Kong and H. Zhang, *Small*, 2013, **9**, 3433-3438.
31. L. Liu, *J. Power Sources*, 2013, **239**, 24-29.
32. C.-Y. Chen, Z.-Y. Shih, Z. Yang and H.-T. Chang, *J. Power Sources*, 2012, **215**, 43-47.
33. Z. Jiang, W. Lu, Z. Li, K. H. Ho, X. Li, X. Jiao and D. Chen, *J. Mater. Chem. A*, 2014, **2**, 8603-8606.
34. D. Kong, H. Wang, Z. Lu and Y. Cui, *J. Am. Chem. Soc.*, 2014, **136**, 4897-4900.
35. E.A.Baranova, A. Cally, A. Allagui, S. Ntais and R. Wuthrich, *C. R. Chimie*, 2013, **16**, 28-33.